Network 2 (1991) 489–509. Printed in the UK

Summation and multiplication: two distinct operation domains of leaky integrate-and-fire neurons

Guido Bugmann

NEC Fundamental Research Laboratories, 34 Miyukigaoka, Tsukuba-Ibaraki 305, Japan

Received 3 June 1991

Abstract. The spiking frequency of a leaky integrate-and-fire (LIF) neuron can be proportional to the sum or the product of a number $n \geqslant 2$ of input frequencies. In this paper, the parameter domains (discharge time constants and synaptic weights) for these two operation modes are defined theoretically and studied by simulations. Summation is based on the frequency division principle and requires discharge time constant as long as possible. In this mode, the LIF neuron is subject to phase locking effects and is insensitive to the irregularity of the input spike trains. Multiplication is based on coincidence detection and requires shorter time constants. Simulations show that the quality of the multiplication function decreases for large irregularities of the input spike trains, that there is an optimum value of the synaptic weights and that there is a consequent input–output frequency level drop. In the brain, the frequency level decrease observed from retina to higher cortical areas might indicate the presence of multiplication-type layers. Physiologically, distant synapses are probably mainly involved in summation while proximal synapses are used for multiplication. It is proposed that learning involves synaptic relocation as well as weights modification.

1. Introduction

The selectivity and generalization power of the visual system is believed to be based on multiplication and summation operations performed on the visual information (Barlow 1969). Most models of motion detection use summation (Reichardt *et al* 1989). There is also indirect physiological evidence that multiplications are performed (for a review, see (Koch and Poggio 1991). However, there is no direct experimental evidence that individual neurons can realize such operations because it is very difficult to determine the actual inputs to a neuron.

In order to determine the computational capabilities of the neurons we study a simulated model of a neuron for which the inputs can be well controlled. We use a leaky integrate-and-fire model (LIF neuron) which emulate first-order, time-independent characteristics of real neurons. Second-order-statistics-dependent synaptic efficiencies (Tsukada *et al* 1976, Braamhof 1991) or long-lasting afterhyperpolarization (Gustafson and Wigstrom, 1981) are not included. Due to these simplifications, the study of LIF neurons provides information on the basic computational capabilities of real neurons. It contributes also to the interpretation of physiological data in term of computational functions. Further, LIF neurons are interesting as possible devices.

Among the few studies on the computational capabilities of LIF neurons, only one covers the multiplication of the input frequencies, and this is in the limited case of two inputs (Srinivasan and Bernard 1976). There are no reports on summation.

0954-898X/91/040489+21$03.50

In this paper, we develop the theoretical expressions defining the parameter domain (synaptic weights, time constants) in which LIF neurons are realizing summation and multiplications. These operations are demonstrated by simulations with LIF neurons whose parameters are chosen to be similar to those of pyramidal neurons.

Each spike of an LIF neuron is, in most cases, produced by only one spike from each input which must arrive within a time window of the order of the discharge time constant. Therefore, the timing of individual spikes is the only relevant information for LIF neurons (Rolls 1990, Abeles *et al* 1990, Bugmann 1991). Neverthless it is convenient to use the input–output relations of the firing frequencies to describe the neuronal function.

It is shown that the decay time of the excitatory postsynaptic potentials (EPSPs) is a crucial factor for determining the neuronal function and that distant synapses are probably mainly involved in summation while proximal synapses are used for multiplication.

An analysis of the parameter domains shows that, with regard to learning, synaptic weights modifications are most likely combined with synaptic relocation.

Pure multiplication could provide very selective information on the presence or absence of a given input pattern but the simulations show that the selectivity decreases as the irregularity of the input spike trains increases.

Finally, the correspondence between the transfer functions of the LIF neurons and formal neurons (Hopfield 1984) is discussed.

A list of symbols appears at the end of the text.

2. The model of a neuron

The LIF neuron (figure 1) is a leaky capacitor being charged by square current pulses initiated by input spikes. The time course of the potential corresponds to the addition of EPSPs originating all at the same electrotonic distance from the soma. The discharge time constant, RC, corresponds to the apparent decay time of the physiological EPSPs. To simulate cortical pyramidal neurons the following parameters are chosen: duration of current pulse $D_s = 1$ ms; threshold potential $V_{th} = 15$ mV; capacitance $C = 6 \times 10^{-11}$ F. The synaptic weights W_{ij} are the amplitudes of the pulses and are given in units of current (nA). When the potential of the capacitor exceeds the threshold potential, the capacitor is reset, an output spike and a refractory time $T_r = 1.5$ ms are initiated. At the end of the refractory time, the potential on the capacitor can again increase. The simulations are performed on the NEC SX-2 supercomputer.

The duration of the refractory time T_r is smaller than that used in some other simulations (Koch and Brunner 1988, Wilson and Bower 1989) and comparable to that used by Harmon (1961) and Amit *et al* (1990). It enables a maximum firing frequency of $1/T_r = 667$ Hz. This is very high compared to usual responses during physiological measurements (10–80 Hz) in the cortex (Rodman *et al* 1989, Georgopoulos *et al* 1984) but is comparable to the maximum frequencies reported in cortical cells (300–900 Hz) (Steriade 1984) during afterhyperpolarization rebounds. These demonstrate the intrinsic capability of cortical neurons to fire at a high rate. Most 'regular spiking' neurons can respond to continuous inputs with similar frequencies during a short time, before adaptation mechanisms have set in (Gustafson and Wigstrom 1981, Connors and Gutnick 1990).

The capacitance of the soma is set to $C = 6 \times 10^{-11}$ F, in accordance with known

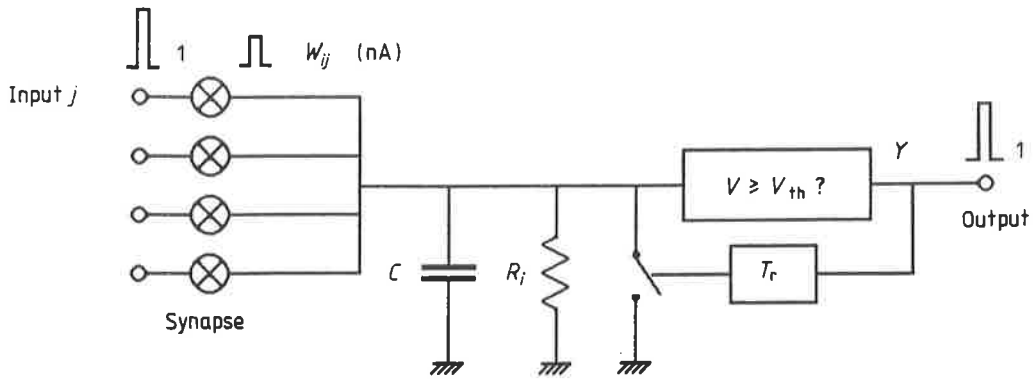

Figure 1. Diagram of the simulated leaky integrate-and-fire (LIF) model of the neuron. The elements of the diagram are described in the text.

neural membrane capacitances ($1-2\,\mu F\,cm^{-2}$ (Jack 1979, Kawato *et al* 1984)) and surfaces of the soma of pyramidal cells ($200-700\,\mu m^2$ (Hillman 1979)).

The threshold voltage of $V_{th} = 15$ mV is near to the average threshold of 19 mV found in rat cortical cells (Wolfson *et al* 1989) and lies between the threshold of the axon's initial segment and the threshold for the somatic sodium conductance (Schwindt and Crill 1982).

The duration $D_s = 1$ ms of the spike-induced postsynaptic input current is assumed to be equal to the presynaptic spike width of 'regular firing' pyramidal neurons (Wolfson *et al* 1989).

During the input current pulse, the postsynaptic potential increases according to classical equations for *RC* circuits (equation (3.2)). After the end of the spike, the potential decreases exponentially with a time constant *RC*. This may be an acceptable approximation for real EPSPs induced by inputs at short electrotonic distances from the soma (Redman 1986, Stratford *et al* 1989). Our model does not comprise the delayed rising phase of the EPSPs initiated on distant dendrites but may reproduce effects related to the slow decay of the later part of these EPSPs.

The input spike trains are produced with a mean frequency f_j and a standard deviation σ_{T_j} on their interspike interval in the following way. After a spike has been produced at time t_n, the time t_{n+1} of the next spike is chosen by:

$$t_{n+1} = t_n + (1/f_j) + \text{RND}(\sigma_{T_j}) \tag{2.1}$$

where $\text{RND}(\sigma_{T_j})$ is a random number generated with a normal distribution centred on zero and a standard deviation $\sigma_{T_j} = \text{RSD}_j/f_j$. RSD_j is the relative standard deviation of the interspike interval also called the 'coefficient of variation of the interspike interval' (Srinivasan and Bernard 1976). It is a measure of the irregularity (sometimes also called 'noise') of the spike trains. An additional constraint is used to prevent the next spike from starting before the end of the refractory time of the preceding one. This procedure produces asynchronous jitter in the timing of spikes with an RSD_j up to 80%.

In case of a continuous input current I, the output frequency $f(I)$ of the LIF neuron is given by:

$$f(I) = 1/\{T_r + RC \ln [IR/(IR - V_{th})]\}. \tag{2.2}$$

Due to the leak, no spike can be initiated by a continuous input current under a threshold $I_{th} = V_{th}/R$ (figure 2). In case of a fluctuating input current produced by spike

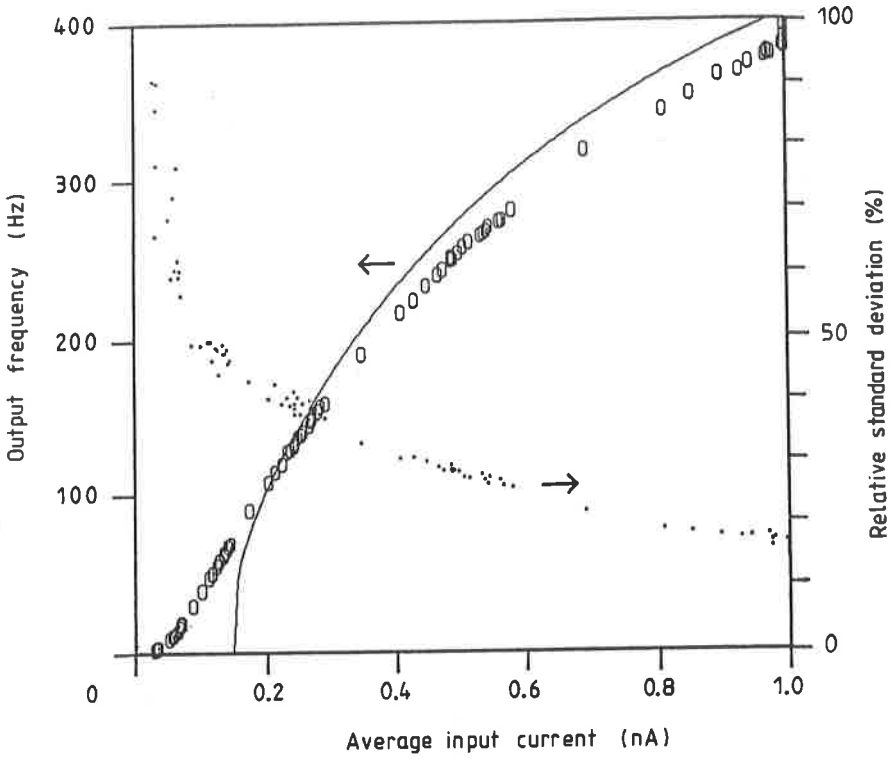

Figure 2. Full line: theoretical transfer function $f(I)$ given by equation (2.2) in the case of a continuous input current I. (O): transfer function obtained from the simulation of 20 spike trains as input. The x-axis represents the average input current (3.13). Due to the fluctuating input current, spikes can be produced at average currents below the threshold I_{th} (in this case $I_{th} = 0.15$ nA) and the charge losses due to the refractory time are enhanced at higher frequencies. (●) relative standard deviation RSD $= \sigma_{T_i}/T_i$ of the interspike intervals of the output spike train. The irregularity of the output spike train is due to the fluctuation of the input current.

trains, the output frequency has a sigmoid-type dependence on the average input current (figure 2). Other characteristics of that model are described elsewhere (Bugmann 1991).

3. Summation mode

3.1. Definition

A LIF neuron i realizes the summation operation when its output frequency f_i is proportional to the sum of the input frequencies f_j:

$$f_i = \frac{1}{k} \sum_{j=1}^{n} f_j \tag{3.1}$$

where n is the number of neurons connected to the input of neuron i and $1/k$ is a constant of proportionality.

When $k = 1$, the neuron realizes summation in the classical sense. In this case, each input spike must produces an output spike and ΔV_+, the potential gain of the capacitor, must reach the threshold voltage V_{th} during the duration D_s of one input spike:

$$\Delta V_+ = W_{ij} R \left(1 - \exp\left(-\frac{D_s}{RC}\right)\right) \geqslant V_{th}. \tag{3.2}$$

Thus the minimum amplitude W_1 for each input spike is:

$$W_1 = V_{th}/[R(1 - e^{-D_s/RC})]. \tag{3.3}$$

In practice (figure 3), the frequency corresponding to the classical summation cannot be reached. This is for instance due to the possible overlapping of two input spikes which leads to only one output spike or to input spikes whose current is partly lost during the refractory time.

In all cases where $k < n$ the maximum f_n of the output frequency is n/k times higher than the maximum f_{in} of the input frequencies f_j. This may lead to an undesirable divergence of a network. On the other hand, there are cases, for instance after a multiplication operation (section 4.4), where we may want to regenerate the frequency level. Therefore, the cases $k < n$ define the 'regenerative summation mode'. In the case $k = n$, the maximum output frequency is equal to the maximum input frequency. This defines the 'equilibrated summation mode'. The constraints on the values of k are described in section 3.3.

3.2. Summation equation

Summation is based on the frequency division principle. For instance, the frequency of a single input spike train is divided by k if we produce one output spike each time k spikes have arrived. For the summation mode, we extend that principle to many input spike trains, producing an output spike each time that k spikes have arrived, regardless of their origin. Thus, the *sum* of the input frequencies is divided by k.

To establish the summation equation, we will use a two-stage approach. First we will determine for which parameters the frequency division is realized in the case of inputs firing all at their maximum frequency $f_{in} = 1/T_{in}$. Later (section 3.4), we will consider the case of lower input frequencies. For the first stage, we assume that: (1) the synaptic weights W_{ij} are all equal; (2) the n input spike trains are made of regularly spaced spikes (RSD = 0%). Our approach consists of requiring that k spikes be able to charge the capacitor to V_{th} when the phase relationships between input spike trains are the least favourable for charging a leaky capacitor, i.e. when there is an equal delay between input spikes. If we establish conditions for summation to work in that case, then it will also work for all the other configurations.

The case of equally spaced input spikes has a zero probability to occur and we will therefore define as the 'most unfavourable case' all configurations of *nearly* equally spaced spikes which have a probability of less than ε to occur. Nearly equally spaced spikes are spikes arriving in equally spaced *time windows* with duration τ. This causes a maximum jitter $\pm\tau$ in the interspike spacings Δt. The probability $P(n, \tau)$ that n input spikes arrive each in a given time window τ is:

$$P(n, \tau) = (\tau f_{in})^n. \tag{3.4}$$

The largest time window τ corresponding to a probability ε is then given by:

$$\tau = (1/f_{in})\varepsilon^{1/n}. \tag{3.5}$$

For our purpose, we will use $\varepsilon = 0.3\%$. This leads to an equation ensuring that summation occurs in 99.7% of all possible cases. Events with occurrence probabilities of more than 99.7% are usually considered as certain (Zayezdny *et al*, 1989). The time window increases when the number of input increases.

To evaluate the potential increase due to the successive input spikes, let us suppose

that the neuron has just fired (for instance after the last of k input spikes), so that its potential is zero. If the delay to the next spike is large enough, the first input spike will arrive after the refractory time which can therefore be neglected. Let us suppose this is the case. At the end of the first input spike, the potential will have increased up to $V_1 = \Delta V_+$ (3.2). After that, the potential decreases due to the leaks and would reach V_{01} at the end of the second spike:

$$V_{01} = V_1 e^{-(\Delta t_1/RC)} \tag{3.6}$$

where Δt_1 is the time separating the first and second input spike. We can write $\Delta t_1 = \Delta t_0 + \delta t_1$, where $\Delta t_0 = T_{in}/n$ is the average delay between two input spikes and δt_1 is the fluctuation of that delay. As the capacitor is also charged by the second spike, its potential reaches in fact $V_2 = V_{01} + \Delta V_+$ at the end of the second spike. There is therefore a gradual gain in potential and, at the end of the kth input spike, the potential has reached V_k which we would like to be at least equal to V_{th}:

$$V_k = \Delta V_+ \left\{ 1 + \sum_{m=1}^{k-1} \exp\left[-\frac{1}{RC}\left((k-m)\frac{T_{in}}{n} + \sum_{j=m}^{k-1} \delta t_j \right) \right] \right\} \geqslant V_{th}. \tag{3.7}$$

As each spike is located in a given time window, the sum of the fluctuations cannot exceed $\pm\tau$. The average value of the fluctuation term is:

$$\overline{\exp\left(-\frac{1}{RC} \sum_{j=m}^{k-1} \delta t_j \right)} = \frac{RC}{2\tau} \int_{-\tau/RC}^{+\tau/RC} e^{-x}\,dx = \frac{RC}{\tau} \sinh\left(\frac{\tau}{RC} \right). \tag{3.8}$$

Using (3.8), equation (3.7) becomes:

$$V_k = \Delta V_+ \left[1 + \frac{RC}{\tau} \sinh\left(\frac{\tau}{RC} \right) \sum_{m=1}^{k-1} \exp\left(-(k-m)\frac{T_{in}}{nRC} \right) \right] \geqslant V_{th} \tag{3.9}$$

The fluctuations of the interspike intervals result in a net potential gain compared to the case of exactly equally spaced spikes ($\sinh(x)/x \geqslant 1$ for $x \geqslant 0$). This is because the increase of the charge leaks during the longer Δt's does not fully compensate for the smaller leaks during the short Δt's.

By using ΔV_+ from (3.2) and τ from (3.5), equation (3.9) defines, for each value of the time constant (RC), the minimum weights allowing the LIF neuron to operate in the summation mode. To find the minimum time constants, knowing the weights, a recursive minimization procedure can be applied.

Equation (3.9) ensures that the LIF neuron fires with a maximum frequency $f_n = (n/k)f_{in}$ when n inputs fire at their maximum frequency f_{in}. This does not imply that its transfer function is linear, i.e. that it would fire at $f_n(n'/n)$ when only n' inputs are active ($n' < n$). To ensure a linear transfer function, the definition of T_{in} in (3.9) must be modified. The longer delays between each of the k spikes when only n' inputs are active are taken into account by replacing T_{in} by T_{in}' defined by:

$$T_{in}' = (n/n')T_{in}. \tag{3.10}$$

In this way, the minimum number n' of inputs for which a linear transfer function is required can be chosen. An example of a transfer function in the case $n' = 2$ is shown in figure 4.

Equation (3.9) has no solution when the weights are smaller than:

$$W_{min} = V_{th} C/(kD_s). \tag{3.11}$$

For smaller weights, even if there are no leaks, k input spikes would not carry enough current to charge the membrane to V_{th} and summation would not be possible. This causes the threshold values of the total current in figure 10.

The equations related to summation can also apply to the average weight as long as individual weights are restricted to values such that any group of k input spikes be able to trigger an output spike. Further, no weights must be larger than W_1 (3.3) since single input spikes would induce output spikes, making frequency division impossible.

The values of the time constants and the weights satisfying (3.9) define a curve in the parameter space shown in figure 10 in the case of the equilibrated summation mode ($k = n$). For a given total weight nW_{ij}, the time constants decrease as the number of inputs decreases.

The physiological counterpart of the potential increase ΔV_+ due to the arrival of one spike is the amplitude of the EPSP measured at the level of the soma. ΔV_+ does not depend much on the decay time and is approximately equal to (from equation (3.2)):

$$\Delta V_+ = \frac{W_{ij} D_s}{C}. \tag{3.12}$$

In figure 10, decay times of 40 ms and more correspond to values of $T_{in}/RC \leqslant 0.5$. The weights are then slightly above minimum and ΔV_+ is roughly equal to V_{th}/k.

3.3. Phase locking effects

The summation equation allows us to determine which number k of input spikes will be necessary to produce an output spike. In such an operation mode, the output frequency can only be an integer fraction $1/k$ of the sum of the input frequencies. In case of a single-input spike train this leads to the well known phase locking effect (Bak 1986, Okajima *et al* 1990) which has been observed in giant squid axons (Matsumoto *et al* 1987). This effect is reported here for the first time in the case of multiple inputs. For instance, in figure 3, we can see that for all weights above 0.91 nA, the output frequency is limited to the total input frequency (case $k = 1$). This is because, even for large weights, the neuron cannot produce more output spikes than the number of input spikes. Below 0.91 nA, one input spike can no more trigger an output spike by itself and two input spikes are necessary, even if the charge carried by the second spike is only partly used. The output frequency is then limited to the half of the total input frequency ($k = 2$).

Some modes are, however, unstable. For instance, the $k = 3$ mode is expected, according to (3.9), for weights between 0.55 nA and 0.45 nA. As 0.91 nA is the minimum weight for one input spike to trigger an output spike, two spikes with weights around 0.5 nA and which are separated by a short delay can also trigger a spike. In case of regular input spike trains, their relative phases therefore play a critical role and modes corresponding to $k = 4, 3, 8/3$ and 2 can be observed (In the $k = 8/3$ mode, three output spikes are produced by a sequence of three, three and two input spikes). In case of noisy input spike trains, there is a random occurrence of favourable or less favourable sequences of spikes and a pure mode $k = 3$ does never occur. This can be seen in figure 3. The mode $k = 4$, which is expected in the range $W_{ij} = 0.4$–0.45 nA is again stable. Higher modes may also be unstable, but, anyway, are difficult to see because of their narrow weight ranges. These observations show that some integer values of k are not accessible in real systems but also that k can be a rational number.

An interesting consequence of phase locking effects is that changes in synaptic weights do not systematically lead to changes in output frequency. For instance, in the

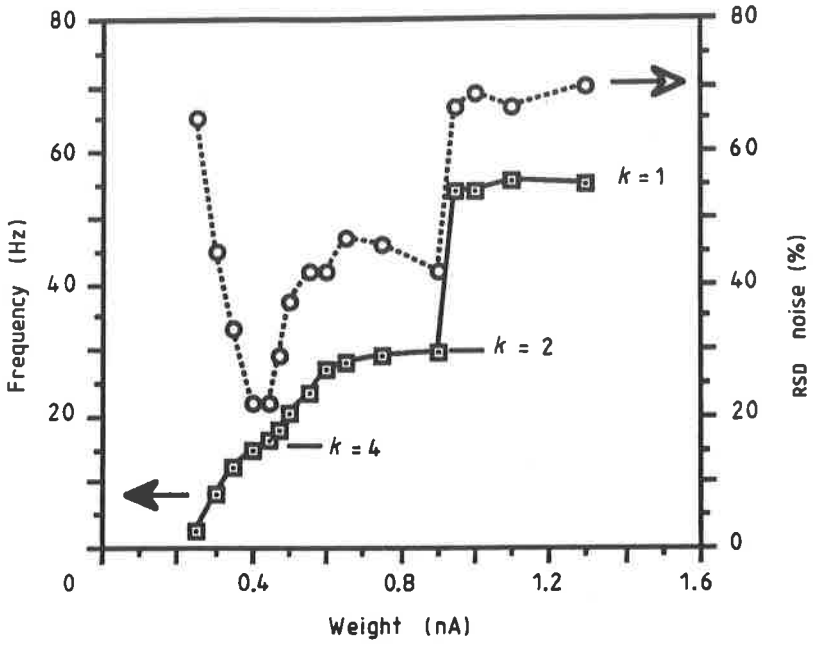

Figure 3. LIF neuron in the summation mode. □ output frequency in case of 4 inputs at $f_j = 15$ Hz. ○ RDS irregularity of the output spike trains. The output frequency is equal to nf_j/k. The modes $k = 1,2$ and 4 are clearly visible. The irregularity RDS of the spike trains is larger than the input irregularity except for $k = n$. Simulation conditions: Input noise: RSD = 20%, spikes counting time: 10 s, $R = 600\,\text{M}\Omega$ ($RC = 36$ ms).

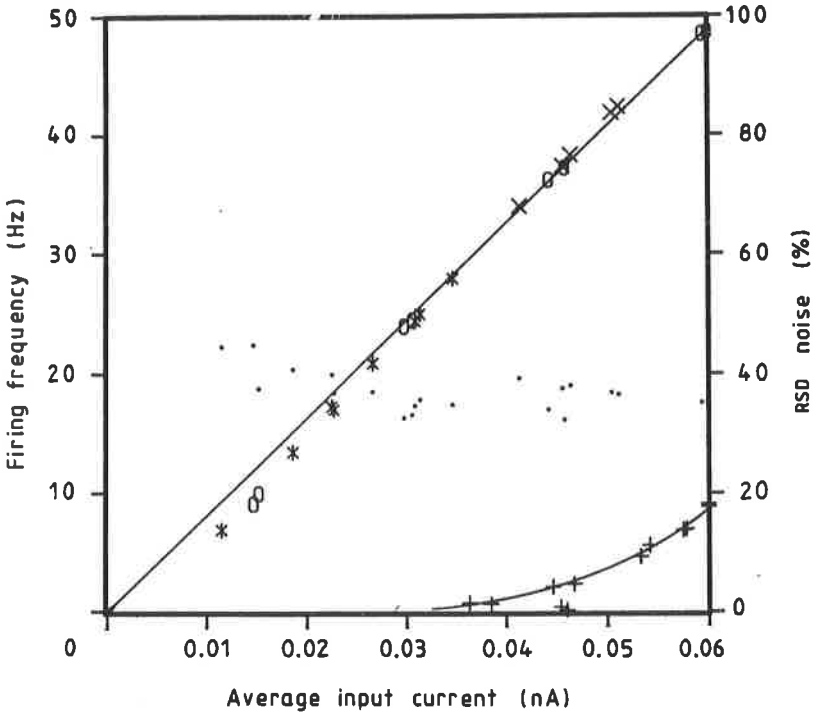

Figure 4. Transfer function in the equilibrated summation mode. (O) 1,2,3 and 4 inputs firing at $f_j = 50$ Hz ($T_{\text{in}} = 20$ ms), $W_{ij} = 0.3$ nA. (*) 4 inputs with frequencies f_j chosen at random in the range 0–50 Hz, $W_{ij} = 0.3$ nA. (×) 4 inputs with f_j's in the range 30–50 Hz. $W_{ij} = 0.15$–0.45 nA (mean: 0.3 nA). (●) RSD of the putput spike trains. (+) Data of figure 7(*a*), in the multiplication mode. Simulation conditions: The leak resistance $R = 1280\,\text{M}\Omega$ ($RC = 77$ ms) has been chosen according to equations (3.9) and (3.10) with $n' = 2$. Due to the choice of $n' = 2$, there is a linear relationship between the output frequencies f_4, f_3 and f_2 but not f_1. The RSD input noise is 60% in all cases. The spikes counting time was 20 s.

case $k = 2$ of figure 3, the weights can be modified in a relatively wide range without any effect on the function of the neuron.

3.4. Transfer function in the summation mode

The averaged input current I_{AV} to a LIF neuron is:

$$I_{AV} = \sum_{j=1}^{n} W_{ij} f_j D_s. \tag{3.13}$$

In the case of equal input weights, the average input current is proportional to the sum of the input frequencies and the output frequency should be proportional to the average input current. This is confirmed by the result of the simulation with various input frequencies and number of inputs (figure 4).

Although the LIF neuron no longer realizes a true frequency summation when the weights are unequal, we have also simulated this case: variable frequencies, variable weights with same average as in the two preceding cases, fixed number of inputs. The results of this simulation define the same transfer function as in the two preceding cases (figure 4).

It can be shown that, in case of unequal weights and $R = \infty$, the transfer function is determined by the average value of the weights (Bugmann, unpublished results). The present simulations indicate that this is also the case with finite leaks. Therefore we propose that, in general, the output frequency of a LIF neuron with parameters set for the summation mode is equal to the weighted average of the input frequencies:

$$f_i = \left(\frac{n}{k}\right)\left(\sum_{j=1}^{n} W_{ij} f_j\right)\left(\sum_{j=1}^{n} W_{ij}\right)^{-1} \tag{3.14}$$

where k depends on the average weights (see section 3.3).

3.5. Irregularity of the spike trains

In the summation mode, the transfer function of the LIF neuron seems to be insensitive to noise. For instance, simulations with an input RSD = 20% produce the same curves as those performed with an RSD = 60% (figure 4).

The irregularity of the output spike trains increases slightly as the frequency decreases (figure 4). It is generally lower than the irregularity of the input spike trains (figure 5) except for very small input noises. In that case there is an intrinsic irregularity due to the unequal input frequencies.

4. Multiplication mode

4.1. Basic mechanism: coincidence detection

In the multiplication mode we expect the output frequency f_i to be proportional to the product of the input frequencies f_j. Such a behaviour can be expected if the neuron operates as a coincidence detector. This means that an output spike is produced each time that n input spikes have arrived each from a different source during a time window τ. By choosing a τ smaller than the smallest input interspike interval we can ensure that the

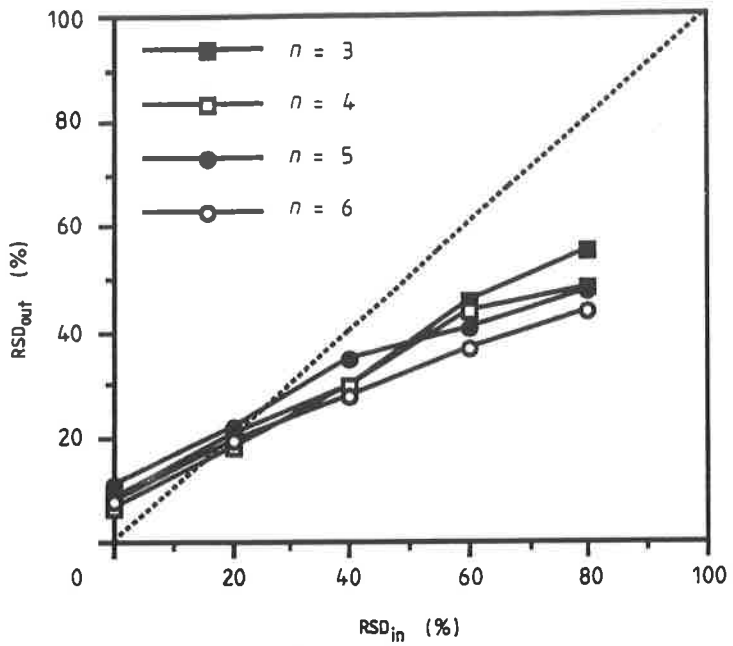

Figure 5. Summation mode: Irregularity RSD_{out} of the output spike trains in dependence on the irregularity RSD_{in} of the input spike trains for the indicated number n of inputs. Simulation conditions: f_j chosen at random in the range 40–50 Hz, all W_{ij} equal, $nW_{ij} = 1.2$ nA. $R = 1280$ MΩ. Spikes counting time: 1 s. Simulations with 5 different sets of f_j are performed and the largest RSD_{out} is displayed. The maximum output frequencies were near to 45 Hz.

n spikes have distinct sources. The probability $P(n, \tau)$ that all n spikes meet during τ is the product of the probabilities P_j that one spike from input j is present during τ:

$$P(n, \tau) = \prod_{j=1}^{n} P_j \tag{4.1}$$

where

$$P_j = f_j \tau. \tag{4.2}$$

If each coincidence leads to an output spike, the output firing frequency of neuron i is given by:

$$f_i = P(n, \tau)/\tau \tag{4.3}$$

or, when combining (4.3), (4.2) and (4.1), by

$$f_i = \tau^{n-1} \prod_{j=1}^{n} f_j. \tag{4.4}$$

Equation (4.4) predicts the output frequency of a device producing spikes as a function of the number of spikes which have arrived during the preceding τ seconds. A LIF neuron is a different device, detecting peaks of the membrane potential. These peaks are indeed highest in the case of coincident inputs but depend also on the past history of non-coincident inputs. Therefore, the LIF neuron cannot realize a pure coincidence detection and there is, to our knowledge, no theory predicting the value of τ for such neurons. However, there is a parameter domain for which the LIF neuron can approximate the multiplication function relatively well.

4.2. Multiplication equation

In case equation (4.4) is satisfied, f_i should drop to zero if one of the inputs does not fire. To establish the multiplication equation, we suppose that $n-1$ inputs provide regular spike trains at a maximum frequency f_{in} and require that almost all the possible combinations of phases are unable to induce output spikes (see section 3.2). The remaining fraction ε of the combinations is composed of the most effective ones for charging a leaky capacitor, namely synchronous spikes.

The probability $P(n-1,\tau)$ that $n-1$ spikes arrive in a time window τ is given by (4.1). Conversely, the time window $\tau(n-1)$ corresponding to a probability ε is given by:

$$\tau(n-1) = \frac{1}{f_{in}} \varepsilon^{1/(n-1)}. \tag{4.5}$$

A spike is considered to arrive during that time window if one of its characteristic parts, for instance the centre, falls within that time window. By simulating the random placement of $n-1$ spikes in a given time window $\tau(n-1)$, we have found that the average delay τ_m between the centres of the first and last spikes was approximately given by:

$$\tau_m = \tau(n-1)[1.035 - 1.1(n-1)^{-0.7}]. \tag{4.6}$$

In the time window τ_m the $n-1$ spikes can take various configurations which, according to our assumptions, are all capable of inducing an output spike. To define the limits of the domain of parameters allowing multiplication, we will require that the least effective among them, namely that of equally spaced spikes, be just insufficiently effective to induce a spike. In this configuration the spikes induce a potential increase V_{n-1} which can be calculated by the methods developed in section 3.2. The interspike delay fluctuates between $\tau(n-1)/(n-2)$ and $[2\tau_m - \tau(n-1)]/(n-2)$ with an average $\tau_m/(n-2)$. This leads to:

$$V_{n-1} = \Delta V_+ \left[1 + \frac{(n-2)RC}{[\tau(n-1) - \tau_m]} \sinh\left(\frac{[\tau(n-1) - \tau_m]}{(n-2)RC} \right) \sum_{m=1}^{n-2} \exp\left(-\frac{m\tau_m}{(n-2)RC} \right) \right] \tag{4.7}$$

where ΔV_+ is given by (3.2). That potential will add to the potential V_0 remaining from the preceding group of spikes which can be at most:

$$V_0 = V_{th} \exp^{-T_{in}/RC} \tag{4.8}$$

where $T_{in} = 1/f_{in}$ is the delay between two time windows. When there is no spiking, the following inequality is satisfied:

$$V_{n-1} + V_0 \leqslant V_{th}. \tag{4.9}$$

This is the multiplication equation based on the assumption of regular spike trains. The effect of irregular input spike trains is discussed below, in section 4.3. In the terms of equation (4.9), the time constant RC appears at various functional levels and a recursive minimization procedure can be used to determine it. The curves of the time constants satisfying (4.9) for various number of inputs are shown in figure 10.

There is no upper limit for the weights in the multiplication mode, because a large W_{ij} can always be compensated by a small time constant. This is, however, at the cost of a decrease in output frequency (figure 8). Theoretically, there is also no minimum average weight because (4.9) imposes only that no spike be produced by $n-1$ inputs. However, for very small weights, one coincidence of n spikes is no more sufficient to induce a spike

and there is a significant drop in the maximum output frequency (figure 8). Therefore, there is an optimum weight to maximize the output frequency.

Our results differ from those of Srinivasan and Bernard (1976) in the case $n = 2$, where they can be compared. These authors require that a spike be produced by two nearly synchronous input spikes while we impose that no spike be produced by a single spike train. Due to our indirect approach, equation (4.9) better takes into account the charge remaining on the capacitor after unsuccessful inputs and imposes smaller time constants.

4.3. *The sensitivity of the transfer function to noise*

The performance of a LIF neuron as a multiplier can be measured by its coefficient of selectivity S defined by:

$$S = (f_n - f_{n-1})/f_n. \tag{4.10}$$

Where f_n is the output frequency produced when the n inputs fire at the maximum input frequency f_{in}. When the LIF neuron operates as a true multiplier, f_{n-1}, the frequency when one of the inputs is inactive, must fall to zero and $S = 1$. In general, the closer the selectivity is to 1 the better is the multiplier.

An example of the dependence of the selectivity on the input noise is shown in figure 6. The selectivity reaches $S = 0.99$ for RSD = 10%. The transfer functions in the cases RSD = 20% ($S = 0.91$) and RSD = 60% ($S = 0.6$) are shown in figure 7.

Due to an increase of f_{n-1}, the selectivity decreases as the input irregularity increases. This is not due to an increase of the number of coincidences because the simulations show no dependence on the initial phases of the $n - 1$ spike trains. It is rather due to the occurrence of shorter interspike intervals on the same input which increases the

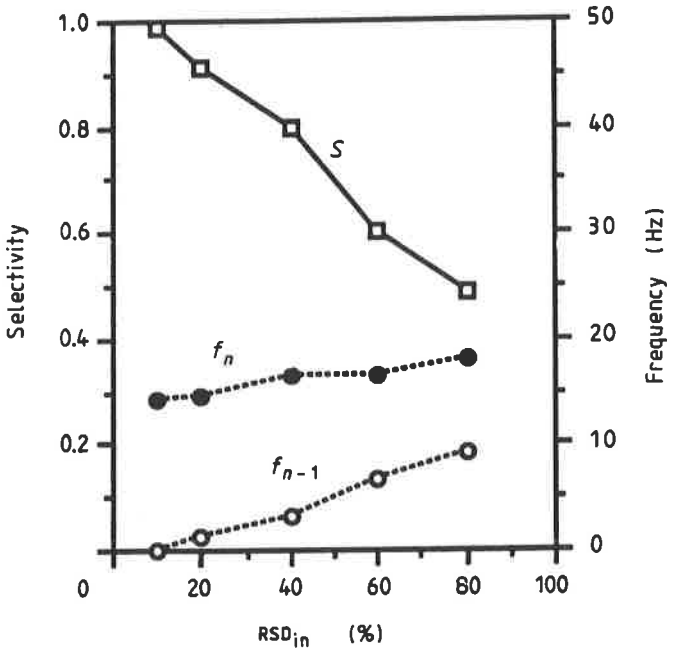

Figure 6. Multiplication mode. Effects of the irregularity RSD of the input spike trains on the selectivity S of a LIF neuron. (□) Selectivity. (●) Frequency f_4. (○) Frequency f_3. Simulation conditions: 3 or 4 inputs firing at 50 Hz, equal weights: $W_{ij} = 0.233$ nA, $RC = 14.4$ ms, spike counting time: 20 s.

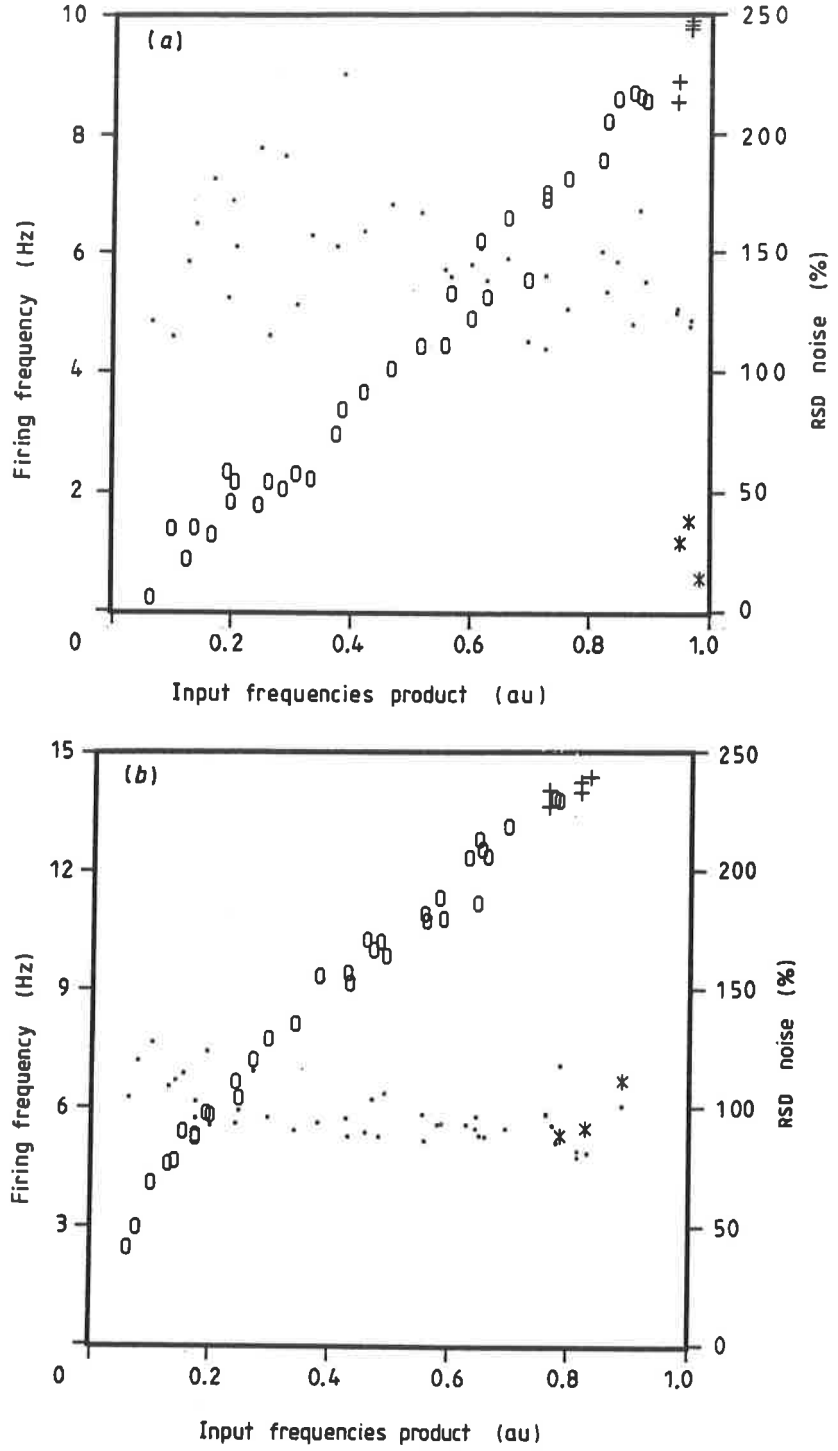

Figure 7. Multiplication mode: Firing frequency in dependence on the product of the normalized input frequencies (f_j/50.5 Hz (*a*); f_j/52 Hz (*b*)) or input noise (*a*) RSD = 20%, (*b*) RSD = 80%. Note the different frequency scales. (+) f_n (f_j = 50 Hz, 4 inputs); (*) f_{n-1} (f_j = 50 Hz, 3 inputs); (O) f_l (f_j = 0–50 Hz, 4 inputs); (●) Irregularity of the output spike trains. Simulation conditions: W_{ij} = 0.3 nA, RC = 7.32 ms (see figure 10), spike counting time: 20 s.

background potential (V_0 in equation (4.9)). The larger the irregularity, the shorter some interspike intervals. It is possible to compensate for this by using smaller values of T_{in} in (4.9) to increase the leaks. Although this operation increases the selectivity, it reduces f_n nearly as effectively as f_{n-1} and the neuron becomes almost silent (Abeles *et al* 1990).

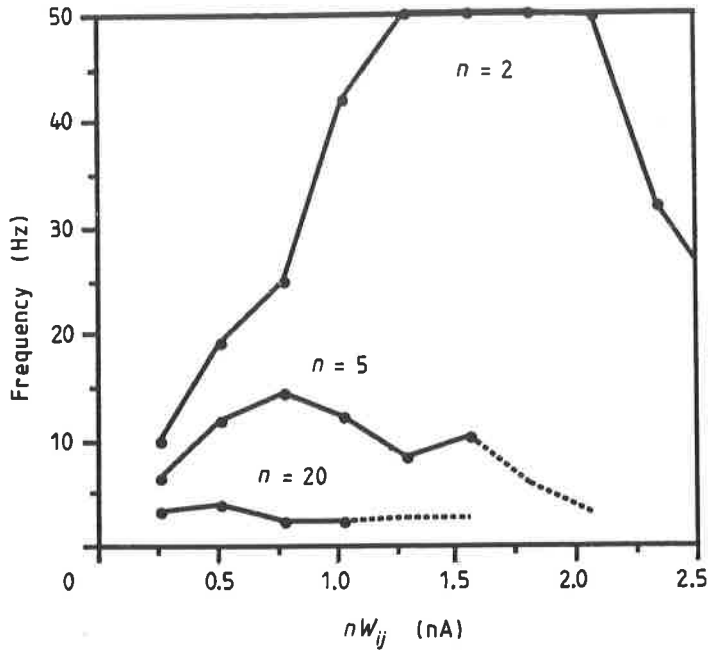

Figure 8. Multiplication mode. Average output frequency in dependence of the total synaptic weights for 2, 5 and 20 inputs. Simulation conditions: input frequencies = 50 Hz; RSD = 0%: spike counting time = 50 × 1 s 50 different random phase relations between input spike trains. (——) Simulations with time constants RC according to theory with $\varepsilon = 0.003$ for $n = 2$ and 5 and $\varepsilon = 0.0001$ for $n = 20$. (– – – –) Best choice of RC to keep $f_{n-1} = 0$ and f_n as high as possible (the theoretical RC's allow non-zero f_{n-1}).

4.4. The output frequency

The output frequency in the multiplication mode shows the maximum discussed in section 4.2 (figure 8). The optimum weight and the maximum output frequency decrease as the number of inputs increases.

For applications of LIF neurons in networks, we may wish that the output frequency of a multiplier falls in the same range as the input frequencies. Actually, this requirement would set the parameters into the equilibrated summation domain (section 3.4) which is compatible with the multiplication mode only in the case $n = 2$ (see figures 8 and 10).

At large weights, f_{n-1} increases when the parameters are set according to the theory. This points to a limitation of the theoretical approach. For the multiplication mode, we allow a fraction ε of the configurations of $n - 1$ nearly simultaneous spikes to induce spikes. However, at large weights there are also configurations of $n - 2$, $n - 3$,... nearly synchronous spikes which become effective. By neglecting these configurations we restrict the validity of the theory to a range of weights decreasing for large n (full lines in figure 8).

4.5. Irregularity of the spike trains

In the multiplication mode, the irregularity of the output spike trains is only slightly higher than in the summation mode when the weights are optimum in the sense of section 4.4 (figure 9). For much larger weights, which must be compensated by small decay times, or for leaks larger than strictly needed for multiplication, as in figure 7, the production of spikes becomes more dependent of true coincidences. These have a low

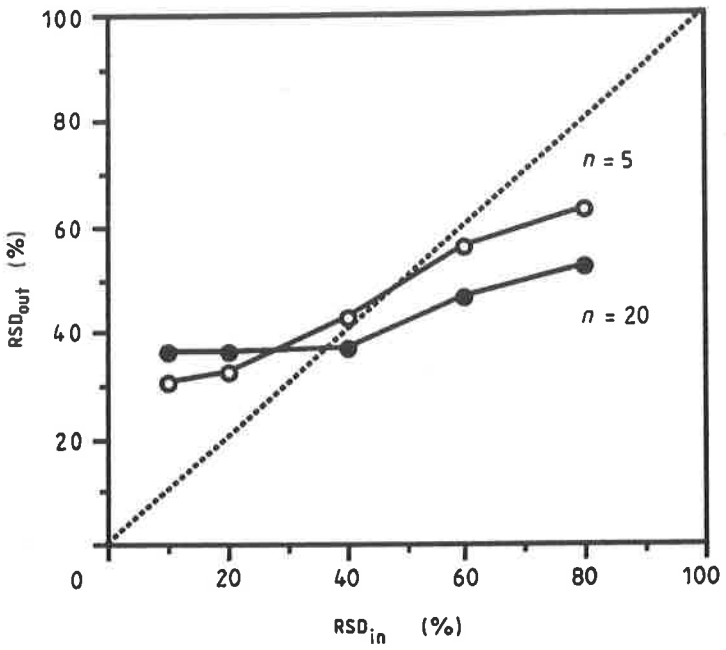

Figure 9. Multiplication mode. Irregularity of the output spike trains in dependence on the input irregularity for 5 and 20 inputs. The curves correspond to the indicated number n of inputs. Simulation conditions: Optimum parameters for multiplication ($n = 5$: $W_{ij} = 0.156$ nA, $RC = 20.1$ ms; $n = 20$: 0.026 nA, 32.7 ms), Input frequency 50 Hz.

probability of occurrence and cause very irregular spike trains. In such cases, values of RSD up to 400% can be observed.

In general, the irregularity of the output spike trains is determined less by the irregularity of the input spike trains than by the frequency of the favourable configurations for spiking. This is exemplified by figure 7.

5. Parameter domains

Our theoretical results are summarized in figure 10. The normalized inverse time constant T_{in}/RC must fall below the dashed lines to set the LIF neuron into the summation mode and above the full lines for the multiplication mode. Except for the case $n = 2$, there is no overlap between the parameters for multiplication and for equilibrated summation. For weights slightly above the summation threshold, the two domains are very close to each other. In this region, the function of a neuron can be modified without changing much the weights and the time constants. With regard to learning of the neuronal function, this is probably the most interesting region.

6. Discussion

To define the domains for multiplication and summation we have used a statistical definition of, respectively, the most and the least effective input configurations. Although it would have been mathematically correct to consider the cases of exactly synchronous spikes for the multiplication equation and exactly equally spaced spikes for the summation equation, the comparison with the result of the simulations led us to

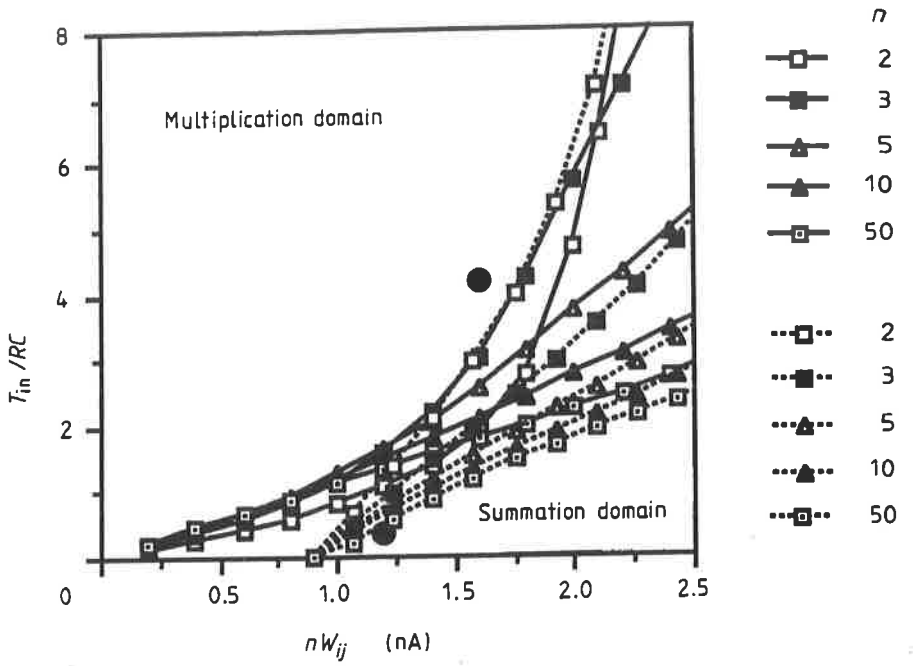

Figure 10. Parameters for summation and multiplication. (----) Normalized inverse time constants calculated with equation (3.9) ($n' = n$) for the equilibrated summation mode ($k = n$) in dependence on the total of the synaptic weights. (——) Normalized inverse of the time constants calculated with the multiplication equation (4.9) ($\varepsilon = 0.01$). (●) Parameters of figures 4 and 7.

introduce the statistical approach. The simulations were performed with a fixed number of input configurations chosen at random, and, as the number of inputs was increased, the exact cases became less and less likely. Therefore, the constraints imposed by equations based on the exact cases were increasingly too strong as the number of inputs was increased. It is, however not straightforward to verify statistical equations because, among the random configurations, some may be closer to the exact case than we assumed by choosing a given ε in the calculations. Therefore, the best fit between simulations and the theory was not always obtained with the same value of ε (figure 8).

Are the parameter domains for summations and multiplications accessible to real neurons?

For input frequencies up to 50 Hz, summation of n inputs requires EPSPs with amplitudes larger than $\frac{1}{n} \cdot 15\,\text{mV}$ (section 3.2). As physiological amplitudes are usually smaller than 1 mV (Redmann 1990), summation would require more than 15 inputs. If the neuron operates near to the minimum weights to minimize its energy consumption, then the decay times should be larger, and possibly much larger, than approximately 40 ms (figure 10). Simulations of passive dendritic propagation show that EPSPs originating at distant synapses have a potential plateau lasting a few tenths of a millisecond followed by a slow decay (Stratford *et al* 1989). If this plateau lasts slightly longer than the delay between two output spikes, then the neuron may behave as if there were an infinite decay time. Physiological observations also show a prolonged decay time for distant inputs (Redman 1986). Therefore, if summation is realized by real neurons, it is most likely mediated by inputs to distant dendrites.

The optimum of the total weights for multiplication ranges from 1.7 nA ($n = 2$) to 0.5 nA ($n = 20$) and is below 0.9 nA for $n \geqslant 4$. The corresponding decay times are 5–40 ms, the smaller decay times corresponding to small numbers of inputs. The shortest

EPSPs are produced by somatic synapses and their decay times are similar to the membrane time constant. This time constant is smaller than 5 ms in cat spinal motorneurons (Jack *et al* 1981, Redman 1986) and 4–15 ms for rat cortical pyramidal cells (Wolfson *et al* 1989, Stratford *et al* 1989). Therefore, if multiplication is realized by real neurons, it is most likely mediated by synapses of intermediate to near electrotonical distances.

As, the optimum parameter domains of the two operation modes are characterized by different decay times and weights, combined changes of weights and decay times are likely to occur during learning in biological systems. While weight modifications have been extensively studied by physiologists (Ito 1989, Bliss and Lynch 1988), decay time changes are not so well documented.

We may note that a neuron in the summation should exhibit a linear temporal response property (Mancini *et al* 1990), because it is a simple spike counter, with no possible facilitation effects related to the history of past inputs. On the contrary, the firing in the multiplication mode is facilitated by other inputs and it should exhibit a nonlinear temporal response property.

The LIF neuron can have any transfer function (TF) between the two extreme operation modes exemplified in figure 4. How can these TF be reproduced with the sigmoid TF of formal neurons? The sigmoid can be shifted horizontally by the bias input so that its lower part can emulate the TF in the multiplication mode. The sigmoid can also be shifted vertically by adding an adequate bias to the output, so that its linear portion emulates the TF in the summation mode. Therefore, formal neurons would need an additional output bias to reproduce the transfer functions of LIF neurons.

LIF neurons operate well below their maximum frequency and show no saturation as do formal neurons. In the normal operation of real neural networks, the problem is probably more to preserve the frequency level than to avoid excessive firing.

What is the role of the synaptic weights in LIF neurons? Although 'weighted summations' can be performed with LIF neurons (3.14), frequency summation is based on a spike counting operation and it does not make much sense to have unequal weights. The multiplication is based on coincidence detection, for which only the probability of spike presence is relevant. If the weights become unequal in such a way that some input spikes can compensate for the absence of others, then the neuron would cease to operate as a multiplier.

Concerning the application of LIF neurons in neural networks, neurons in the multiplication mode are correlation or decision units, strongly affected by the inactivity of any of the inputs and can perform feature extractions. In the summation mode, neurons can realize translation invariance within their receptive field (provided a certain feature can only appear in that field once at a time). A multilayer neural network of alternating summing and multiplying layers, in the spirit of the neocognitron (Fukushima *et al* 1983, Fukushima and Wake 1991), may therefore exhibit many properties of real perception systems. In such a network, the total number of multiplication layer would be limited by the frequency-level drop occurring in each layer.

A decrease in frequency level is also observed in real nervous systems, from periphery to higher centres. In the visual system for instance, firing frequencies of 300 Hz are quite common in the retina (Levick 1973) or in the LGN (Saul and Humphrey 1990) while good responses are near to 80 Hz in V1 and near to 20 Hz in MT (Maunsel and Newsome 1987, Rodmann *et al* 1989). Our results are therefore compatible with the idea that successive feature extraction operations are performed on the visual information.

The operation of LIF neurons as multipliers would be improved by a limitation of the

irregularity of the input spike trains. As the outputs of LIF neurons are irregular, realizing a multilayer neural network of multipliers may represent a serious noise-management problem. It would be interesting to find out how this problem is solved by real nervous systems.

7. Conclusion

We have defined the parameter domain in which LIF neurons can realize the summation and the multiplication of the input frequencies. The transposition of our results to biological neurons suggests that neurons in the summation mode use more distal synapses and EPSPs of larger amplitude than neurons in the multiplication mode.

If we like to think that the actual function of a neuron is activity dependent, then the corresponding learning mechanism should involve not only weight modifications but also synaptic relocation, physical or functional.

Summation is a robust noise-insensitive operation based on frequency division. Multiplication is more complicated to handle, it requires not too noisy input spike trains and shows a frequency drop which makes it difficult to multiply more than 20 inputs. The later phenomena may explain the progressive frequency-level decrease observed along the visual system.

Acknowledgments

We wish to thank S Fujiwara, K Okajima, M Nomura, S Tanaka and M Miyashita for their help, advice and discussions. This work was performed under the management of FED (the R&D Association for Future Electron Devices) as a part of the R&D of Basic Technology for Future Industries, supported by NEDO (New Energy and Industrial Technology Development Organization).

List of symbols

C	Capacitance of the cellular membrane (F)
D_s	Duration of the spikes and inward current pulse (s)
ΔV_+	Membrane potential increase due to input spikes (V)
Δt	Delay between arriving spikes (s)
Δt_0	Average delay between arriving spikes (s)
δt	Fluctuation of the delay between arriving spikes (s)
ε	Probability of a given configuration of phases of the input spike trains
f_i	Output frequency (neuron i is the output neuron) (Hz $= s^{-1}$)
f_{in}	Maximum input frequency (Hz)
f_j	Input frequency (neuron j is an input neuron) (Hz)
f_n	Output frequency of a LIF neuron when n connected inputs fire at their maximum frequency f_{in}(Hz)
$f(I)$	Firing frequency due to a continuous input current I (Hz)
I	Continuous input current (A)
I_{AV}	Time averaged total input current (A)

I_{th}	Threshold below which a continuous input current cannot initiate a spike (A)
k	Number of input spikes necessary to produce an output spike in the summation mode
n	Number of inputs connected to a neuron
n'	Minimum number of active inputs for which the transfer function is linear
P_j	Probability that one spike from neuron j arrives during the time window τ
$P(n, \tau)$	Probability that n input spikes from distinct sources arrive during the time window τ
R	Leak resistance of the membrane (Ω)
RC	Discharge time constant of the membrane ($=R \times C$) (s)
RSD	Relative standard deviation of the interspike intervals ($=\sigma_{T_i}/T_i$)
σ_{T_i}	Standard deviation of the interspike intervals (s)
S	Selectivity of the LIF neuron as a multiplier
τ	Time window for input spikes (s)
τ_m	Mean delay between the first and last spike in the time window τ (s)
T_i	Average interspike interval of the spikes produced by neuron i (s)
T_{in}	Average interspike interval corresponding to the maximum input frequency f_{in} (s)
t_n	Time of occurrence of the spike number n in a spike train (s)
T_r	Duration of the refractory time (starting at same time as an output spike) (s)
V	Potential of the cellular membrane or the capacitor (V)
V_0	Potential remaining from preceding spikes (V)
V_k	Potential at the end of the kth input spike (V)
V_{th}	Threshold potential for spike initiation (V)
W_{ij}	Synaptic weight for inputs from neuron j to neuron i. In this model, the synaptic weight is the amplitude of the input current pulse induced by the spike (A)
W_{min}	Minimum synaptic weight in the summation mode (A)
W_1	Weight allowing a single input spike to induce an output spike (A)

References

Abeles M, Vaadia E and Bergman H 1990 Firing pattern of single units in the prefrontal cortex and neural network models *Network* **1** 13–25

Amit D J, Evans M R and Abeles M 1990 Attractor neural networks with biological probe records *Network* **1** 381–405

Bak P 1986 The devil's staircase *Phys. Today* **39** (December) 38–45

Barlow H B 1969 Trigger features, adaptation and economy of impulses ed K N Leibovic *Information Processing in the Nervous System*, (Berlin: Springer) pp 209–30

Bliss T V P and Lynch M A 1988 Long-term potentiation of synaptic transmission in the hippocampus: properties and mechanisms *Long Term Potentiation: Mechanisms and Key Issues* ed P W Landfield and S A Deadwyler (New York: Liss) pp 3–72

Braamhof M 1991 Spatiotemporal correlation in the cerebellum *Artificial Neural Networks* ed T Kohenen *et al* (Amsterdam: Elsevier) pp 1739–42 (also 1991 *Proc. IJCNN'91 (Seattle)*)

Bugmann G 1991 Neural information carried by one spike *Proc. 2nd Australian Conf. on Neural Networks (ACNN'91), (Sydney)* pp 235–8

Connors B W and Gutnick M J 1990 Intrinsic firing patterns of diverse neocortical neurons *Trends in Neuroscience* **13** 99–104

Fukushima K, Miyake S and Ito T 1983 Neocognitron, a neural network model for a mechanism of visual pattern recognition *IEEE Trans. Systems Man Cybern.* **SMC-13** 826–34

Fukushima K and Wake N 1991 Handwritten character recognition by the neocognitron *IEEE Trans. Neural Networks* **NN-2** 355–65

Georgopoulos A P, Kalaska J F, Crutcher M D, Caminiti R and Massey J T 1984 The representation of movement direction in the motor cortex: single cell and population studies *Dynamic Aspects of Neocortical Function* ed G M Edelmann *et al* (New York: Wiley) pp 501–24

Gustafsson B and Wigstrom H 1981 Shape of frequency-curves in CA1 pyramidal cells in the hippocampus *Brain Res.* **223** 417–21

Harmon L D 1961 Studies with artificial neurons, I: properties and functions of an artificial neuron *Kybernetik* **3** 89–101

Hillman D E 1979 Neural shape parameters and substructures as a basis of neuronal from *The Neurosciences (4th Study Program)* ed F O Schmitt and F G Worden (Cambridge, MA: MIT Press)

Hopfield J J 1984 Neurons with graded response have collective computational properties like those of two-state neurons *Proc. Natl Acad. Sci. USA* **81** 3088–92

Ito M 1989 Long-term depression *Ann. Rev. Neurosci.* **12** 85–102

Jack J 1979 An introduction to linear cable theory *The Neurosciences (4th Study Program)* ed F O Schmitt and F G Worden (Cambridge, MA: MIT Press) pp 423–37

Jack J, Redman S J and Wong K 1981 The components of synaptic potentials evoked in cat spinal motorneurons by impulses in single group Ia afferents *J. Physiol.* **312** 65–96

Kawato M, Hamaguchi T, Murakami F and Tsukahara N 1984 Quantitative analysis of electrical properties of dendritic spines *Biol. Cybern.* **50** 447–54

Koch U T and Brunner M 1988 A modular analog neuron-model for research and teaching *Biol. Cybern.* **59** 303–12

Koch C and Poggio T 1991 Multiplying with synapses and neurons *Single Neuron Computation* ed S Zornetzer *et al* in press

Levick W R 1973 Variation in the response latency of cat retinal ganglion cells *Vision Res.* **13** 837–53

Mancini M, Madden B C and Emerson R C 1990 White noise analysis of temporal response properties in simple cells of cat cortex *Biol. Cybern.* **63** 209–19

Matsumoto G, Takahashi N and Hanyu Y 1987 Chaos, phase locking and bifurcation in normal squid axons *Chaos in biological systems* ed H Deng *et al* (New York: Plenum) pp 143–56

Maunsell J H R and Newsome W T 1987 Visual processing in monkey extrastriate cortex *Ann. Rev. Neurosci.* **10** 363–401

Okajima K, Nomura M, Bugmann G and Fujiwara S 1990 Modeling of visual information processing *Proc. 9th Symp. on Future Electron Devices (Makuhari, Chiba, Japan)* (Research & Development Association for Future Electron Devices, Tokyo) pp 159–66.

Reichardt W, Egelhaaf M and Ai-ke Guo 1989 Processing of figure and background motion in the visual system of the fly *Biol. Cybern.* **61** 327–45

Redman S 1986 Monosynaptic transmission in the spinal cord *News in Physiol. Sci.* **1** 171–4

—— 1990 Quantal analysis of synaptic potentials in neurons of the central nervous system *Physiol. Rev.* **70** 165–98

Rodman H R, Gross C G and Albright T D 1989 Afferent basis of visual response properties in area MT of the macaque. I. Effect of striate cortex removal *J. Neurosci.* **9** 2033–50

Rolls E T 1990 Principles underlying the representation and storage of information in neural networks in the primate hippocampus and cerebral cortex *An Introduction to Neural and Electronic Networks* ed S F Zornetzer *et al* (New York: Academic) pp 73–90

Saul A B and Humphrey A L 1990 Spatial and temporal response properties of lagged and nonlagged cells in cat lateral geniculate nucleus *J. Neurophysiol.* **64** 206–24

Schwindt P C and Crill W E 1982 Factors influencing motorneuron rhythmic firing: results from a voltage clamp study *J. Neurophysiol.* **48** 875–90

Srinivasan M and Bernard G D 1976 A proposed mechanism for multiplication of neural signals *Biol. Cybern.* **21** 227–36

Steriade M 1984 The excitatory–inhibitory response sequence in thalamic and neocortical cells: State-related changes and regulatory systems *Dynamic Aspects of Neocortical Function* ed G M Edelmann *et al* (New York: Wiley) pp 107–57

Stratford K, Mason A, Larkman A, Major G and Jack J 1989 The modelling of pyramidal neurons in the visual cortex *The Computing Neuron* ed R Durbin *et al* (Wokingham: Addison-Wesley) pp 296–321

Tsukada M, Nishi N and Sato R 1976 Stochastic automaton model for the temporal pattern discrimination of nerve impulses sequences *Biol. Cybern.* **21** 121–30

Wilson M A and Bower J M 1989 The simulation of large-scale neural networks *Methods in Neuronal Modeling* ed C Koch and I Segev (Cambridge, MA: MIT Press) pp 291–333

Wolfson B, Gutnick M J and Baldino F Jr 1989 Electrophysiological characteristics of neurons in neocortical explant cultures *Exp. Brain Res.* **76** 122–30

Zayezdny A, Tabak D and Wulich D 1989 *Engineering Application of Stochastic Processes* (New York: Wiley) p 32